International Journal of Pharmaceutics 367 (2009) 179–186

Contents lists available at ScienceDirect

International Journal of Pharmaceutics

journal homepage: www.elsevier.com/locate/ijpharm

Pharmaceutical Nanotechnology

Formulation and pharmacokinetic evaluation of an asulacrine nanocrystalline suspension for intravenous delivery

Srinivas Ganta[a], James W. Paxton[b], Bruce C. Baguley[c], Sanjay Garg[a,*]

[a] School of Pharmacy, The University of Auckland, Private Bag 92019, Auckland, New Zealand
[b] Department of Pharmacology, The University of Auckland, Private Bag 92019, Auckland, New Zealand
[c] Auckland Cancer Society Research Centre, The University of Auckland, Private Bag 92019, Auckland, New Zealand

ARTICLE INFO

Article history:
Received 30 July 2008
Received in revised form 7 September 2008
Accepted 13 September 2008
Available online 21 September 2008

Keywords:
Asulacrine
Nanosuspension
High pressure homogenization
Dissolution
Pharmacokinetics
Tissue distribution

ABSTRACT

Asulacrine (ASL) is an inhibitor of topoisomerase II, which has shown potential against breast and lung cancer. It is a poorly water soluble drug. To allow intravenous (i.v.) administration, ASL was formulated as a nanocrystalline suspension by high pressure homogenization. The nanosuspension was lyophilized to obtain the dry ASL nanoparticles (average size, 133 ± 20 nm), which enhanced both the physical and chemical stability of the ASL nanoparticles. ASL dissolution and saturation solubility were enhanced by the nanosuspension. Differential scanning calorimetry and X-ray diffraction analysis showed that the crystallinity of the ASL was preserved during the high pressure homogenization process. The pharmacokinetics and tissue distribution of ASL administered either as a nanosuspension or as a solution were compared after i.v. administration to mice. In plasma, ASL nanosuspension exhibited a significantly ($P < 0.01$) reduced C_{max} (12.2 ± 1.3 μg ml^{-1} *vs* 18.3 ± 1.0 μg ml^{-1}) and $AUC_{0-\infty}$ (18.7 ± 0.5 μg ml^{-1} h *vs* 46.4 ± 2.6 μg ml^{-1} h), and a significantly ($P < 0.01$) greater volume of distribution (15.5 ± 0.6 l kg^{-1} *vs* 2.5 ± 0.1 l kg^{-1}), clearance (1.6 ± 0.04 l h^{-1} kg^{-1} *vs* 0.6 ± 0.04 l h^{-1} kg^{-1}) and elimination half-life (6.1 ± 0.1 h *vs* 2.7 ± 0.2 h) compared to the ASL solution. In contrast, the ASL nanosuspension resulted in a significantly greater $AUC_{0-\infty}$ in liver, lung and kidney (all $P < 0.01$), but not in heart.

1. Introduction

An increasing number of newly developed drugs are poorly soluble in water as well as in organic media (Lipinski, 2002). As a result, the formulation of these drugs is a major problem in their clinical development. Such drugs often have poor bioavailability because of their extreme low aqueous solubility (Muller and Peters, 1998; Patravale et al., 2004; Rabinow, 2004). New drugs emerging from the drug discovery process often have high molecular weight and high log *P* value, both of which contribute to insolubility (Lipinski et al., 1997). Attempts to solubilise poorly soluble drugs using co-solvents, in micelles, or with cyclodextrins have been of limited success. An alternative approach is the formulation of the poorly soluble drugs as nanosuspensions (Böhm and Muller, 1999). Nanosuspensions are colloidal dispersions of nano-sized drug particles which are produced by an appropriate size-reduction method and stabilized by a suitable stabilizer (Böhm and Muller, 1999; Patravale et al., 2004; Rabinow, 2004). According to Noyes-Whitney and Ostwald-Freundlich principles, particle size in the nanometer range can lead to an increased dissolution velocity and saturation solubility for a nanosuspension, which is usually also accompanied by an increase in bioavailability (Böhm and Muller, 1999; Hintz and Johnson, 1989). An important advantage of the nanosuspension is that they can be given by various routes of administration, such as oral (Liversidge and Cundy, 1995), parenteral (Peters et al., 2000), ocular (Rosario et al., 2002) and pulmonary delivery (Jacobs and Muller, 2002). In addition, due to its small particle size and safe composition, nanosuspension can be injected intravenously (i.v.) to give 100% bioavailability (Muller and Keck, 2004). Nanosuspensions may also show passive targeting similar to colloidal drug carriers after i.v. administration (Peters et al., 2000). Following modification to the surface with special stabilizers, some active targeting may also be achieved *in vivo* with nanosuspensions (Muller and Keck, 2004; Rabinow, 2004).

Particle size reduction to the nanometer range can be achieved through media milling (Merisko-Liversidge et al., 1996) or high pressure homogenization (Muller et al., 2001; Muller and Peters, 1998). The major concern with the former is the generation of residues of milling media, which may be introduced in the final product as a result of erosion (Buchmann et al., 1996). The high pressure homogenization technique has been extensively described with regard to particle size-reduction efficiency (Muller et al., 2001;

* Corresponding author. Tel.: +64 9 373 7599x82836; fax: +64 9 367 7192.
E-mail address: s.garg@auckland.ac.nz (S. Garg).

0378-5173/$ – see front matter © 2008 Elsevier B.V. All rights reserved.
doi:10.1016/j.ijpharm.2008.09.022

Muller and Peters, 1998). As it is very simple, time-saving and is an organic solvent free process, it presents advantages over other milling techniques. However, with high pressure homogenization, the drug particles should be sufficiently small to pass through the homogenization gaps (Muller and Peters, 1998).

Asulacrine (ASL), is a derivative of the anti-leukaemia drug amsacrine, first synthesized in the Auckland Cancer Society Research Centre (Baguley et al., 1984; Cain et al., 1975). It is an inhibitor of topoisomerase II (Schneider et al., 1988), and its anti-tumour action is mediated through DNA breakage and the formation of DNA protein cross-links leading to cell death (Baguley, 1990; Covey et al., 1988). Despite its severe toxicity, ASL has the potential to be effective against breast and lung cancers (Baguley et al., 1984; Sklarin et al., 1992).

ASL is a hydrophobic drug and poorly soluble in water. In this study, high pressure homogenization was evaluated for the ASL nanosuspension preparation for i.v. administration. The ASL nanosuspension was characterized for its particle size distribution and morphology, and its dissolution and solubility properties were determined to confirm theoretical enhancement predictions. The ASL crystalline state was also studied before and following particle size-reduction methods to assess if the initial crystalline state was preserved, which is important for long-term stability. To assess the *in vivo* properties of the ASL nanosuspension, the pharmacokinetics and tissue distribution were investigated in C57 BL/6 mice.

2. Materials and methods

2.1. Materials

Asulacrine (SN 21407) and the corresponding ethylsulphonanilide analogue (SN 23305), for use as an internal standard (I.S.), were provided by the Auckland Cancer Society Research Centre. Anhydrous sodium acetate and propylene glycol were obtained from Scharlau Chemie (Spain) and dimethyl acetamide from Acros Organics (USA). Poloxamer 188 (Pluronic F 68) was kindly provided by BASF (USA). Glycerol and Tween 80 were purchased from Sigma chemicals (St. Louis, USA). HPLC grade acetonitrile and methanol were obtained from Ajax Fine Chemicals (Australia). All other chemicals and reagents were of analytical grade. Water was purified on a Milli-Q system (Millipore, USA), and was used for the preparation of all aqueous solutions.

2.2. Preparation of asulacrine nanosuspension

The ASL nanosuspension was prepared by ultra-turrax homogenization, followed by high pressure homogenization. Poloxamer (1%, w/v) was dissolved in 25 ml of water to obtain the aqueous surfactant solution, which was poured on the ASL (0.5%) powder with continuous mixing. This slurry was then subjected to a pre-homogenization with an ultra-turrax homogenizer (IKA Werke GmbH & Co., Germany) at 15,000 rpm for 15 min under low temperature (2–4 °C). This coarse suspension was then circulated for 10 cycles at 500 bar pressure through the Emulsiflex-C3 high pressure homogenizer (Avestin Inc., Canada), followed by another 10 cycles at 1000 bar as a kind of pre-milling. Finally, the suspension was homogenized for 20 cycles at 1500 bar until an equilibrium size was reached. A continuous cooling via heat exchanger (Refrigerated Circulator, Julabo Labortechnique, GmbH, Germany) was used during the homogenization process to maintain the product temperature between 2 and 4 °C. Samples were withdrawn after the pre-homogenization and homogenization size-reduction steps for size distribution analysis. The nanosuspension was then lyophilized immediately to obtain a dry powder, which was dispensed into glass vials and frozen at −20 °C for 12 h. This was then transferred to a freeze-dryer (Labconco, Labconco Corporation, USA), and dried for 48 h at −55 °C and at a pressure of 0.133 mbar, with a secondary cycle of 5 h with the temperature adjusted to 25 °C. The lyophilized product was then re-dispersed with 2.21% (w/v) of glycerin in water for i.v. administration. Re-dispersion was by manual shaking for 1 min and the re-dispersion volume being equivalent to the original volume of the nanosuspension.

2.3. Characterization of asulacrine nanosuspension

2.3.1. Particle size measurement

The size distribution of the particles in the ASL nanosuspension was determined by a dynamic light scattering (DLS) technique with a Mastersizer 2000 (Malvern Instruments, UK). The nanosuspension samples for particle size analysis were added to the small sample dispersion unit containing water as a dispersant. The refractive index at 1.5 was used for measurements, and the laser obscuration range was maintained between 10 and 20%. Three observations were recorded for each sample. The diameters reported were calculated using volume distribution. The particle size, d(v; 0.5) (size of the particles for which 50% of the sample volume contains particles smaller than d(v; 0.5)), and d(v; 0.9) (size of the particles for which 90% of the sample volume contains particles smaller than d(v; 0.9)) were used as characterization parameters.

2.3.2. Morphology

Morphological evaluation of ASL nanoparticles was conducted by scanning electron microscopy (SEM). The lyophilized nanosuspension samples were placed on a carbon specimen holder, and then coated with platinum in a sputter coater (Polaron SC 7640), and then observed with a Philips XL30S FEG scanning electron microscope (Philips, Eindhoven, Netherlands).

2.3.3. Crystalline state evaluation

Crystalline state evaluation before and following particle size reduction was conducted by differential scanning calorimetry (DSC) and powder X-ray diffraction (PXRD) to indicate any transformation to amorphous state during the high pressure homogenization process. The thermal properties of the ASL and other excipients in the nanosuspension were investigated with a DSC calibrated with indium (calibration standard, purity >99.999%) for melting point and heat of fusion (Shimadzu, Japan). A heating rate of 10 °C/min was employed over the range of 25–300 °C. Samples (approximately 10 mg) were analyzed in standard aluminum sample pans with an empty pan used as a reference. Thermograms of nanosuspension samples and their individual excipients were recorded. PXRD diffractograms of ASL and other excipients in the nanosuspension were recorded using a Brucker AXS diffractometer (Model: D8 Advance) with Cu line as the source of radiation. Standard runs using a 40 kV voltage, a 40 mA current and a scanning rate of 0.02°/min over a 2θ range of 2–40° were used.

2.3.4. Saturation solubility

The saturation solubility evaluation of ASL in nanosuspension was carried out in phosphate buffered saline (PBS) (Na_2HPO_4, 0.017 M; KH_2PO_4, 0.0014 M; and NaCl, 0.1370 M, pH 7.4) at 37 °C. Lyophilized powder was dispersed into these media to obtain 5 mg/ml of drug suspension and placed on a shaking water bath for 48 h. Samples were centrifuged, the resulting supernatant was diluted in a mobile phase and 50 μl volume was injected into the HPLC for analysis.

2.3.5. Dissolution study

A Hanson SR8 Plus dissolution test station (USP apparatus-II, paddle method) operating at a rotation speed of 100 rpm was used for *in vitro* testing of ASL dissolution. All dissolution tests were run in triplicate on an equivalent of 5 mg of ASL in nanosuspension. PBS (pH 7.4) with 1% Tween 80 was used as the dissolution media. The volume and temperature of the dissolution medium were 500 ml and 37 ± 0.5 °C, respectively. At each sampling time, 2 ml was withdrawn using sampling port attached with 0.22 μm filter disc, and 2 ml blank medium was added back into the vessels through the sampling port. Samples were centrifuged, the resulting supernatant was diluted in a mobile phase and 50 μl volume was injected into the HPLC for analysis.

2.3.6. Stability study

Storage stability was studied by storing the lyophilized nanosuspension samples at 4 and 25 °C for up to 3 months. Periodically, samples were removed and the particle size was measured. In addition, ASL stability in the nanosuspension was examined by determining (by HPLC assay) the amount of parent drug remained after specific storage periods.

2.4. Preparation of asulacrine injection solution

The ASL solution was prepared by dissolving 30 mg of ASL in 1 ml of dimethyl acetamide, and then diluting to 2 ml with propylene glycol. This preparation was injected immediately by the i.v. route at an ASL dose of 30 mg/kg body weight. This dose was chosen for the pharmacokinetic study based on its curative activity in mice bearing Lewis lung tumours (Baguley et al., 1984).

2.5. Pharmacokinetics and tissue distribution

Male mice (C57 BL/6) weighing 25–30 g were obtained from the Vernon Jansen Unit, The University of Auckland, New Zealand. The animals were acclimatized for at least 1–2 weeks before experimentation, fed with standard diet, and allowed water *ad libitum*. All animal experiments were evaluated and approved by the Animal Ethics Committee, The University of Auckland, New Zealand. Mice in groups received i.v. injection of ASL (30 mg/kg) in solution (ASL) or nanosuspension (ASL-NS) via the tail vein with a 1CC Tuberculin syringe fitted with a 26 gauge needle. Control groups received the appropriate vehicles. At predetermined time points (5, 15, 30 min and 1, 2, 4, 6, 8 and 13 h), three mice from each group were anaesthetized with isoflurane, blood collected from the retro-orbital sinus into heparin (10 μl, 500 IU/ml) treated tubes, and centrifuged at 3500 rpm for 15 min for the isolation of the plasma. The mice were then euthanized by cervical dislocation, and the liver, kidney, heart, and lungs were collected, washed, weighed and homogenized (Ultra-turrax homogenizer (IKS T10), IKA Werke GmbH & Co., Germany) in 1 ml of PBS (pH 7.4). After collection, both plasma and tissue samples were stored at −20 °C until further analysis.

2.6. Plasma and tissue sample processing

To determine the ASL concentration, I.S. was added to 0.1 ml of plasma or tissue homogenate, followed by 1 ml chilled acetonitrile. Each sample was vortexed for 1 min with a VX100 Labnet vortex mixer (Labnet Int., NJ, US), and then kept on ice for 30 min. After centrifugation (Sigma Laborzentrifugen, Germany) at 3500 rpm for 15 min to precipitate the proteins, the supernatant was removed to clean test tubes and vacuum dried (Labconco Corporation, Kansas, US). Residues were dissolved in 1 ml of mobile phase, and 50 μl aliquots injected into the HPLC for analysis.

2.7. HPLC analysis

A previously reported method from our lab was used for the analysis of ASL in biological samples (Ganta et al., 2008). A Waters® series LC, comprising of a binary pump, an autosampler, and dual wavelength detector were used, with data acquisition by Breeze software (Waters Corporation). The HPLC separation was performed on a Gemini C18 analytical column (250 mm × 4.6 mm, particle size 5 μm) from Phenomenox, USA and a C18 precolumn of the same packing (12.5 mm × 4.6 mm). The mobile phase consisted of 0.01 M sodium acetate buffer, pH 4.0 adjusted with acetic acid and acetonitrile (55:45, v/v). It was filtered through a 0.45 μm nylon filter (Alltech Associates, Inc., Deerfield, IL) and degassed in an ultrasonic bath (Bandelin Electronics, Berlin, Germany) before use. All samples were analyzed under isocratic elution at a flow rate of 1 ml/min, and at a wavelength of 254 nm. The autosampler temperature was maintained at 10 °C, with a 50 μl injection volume.

The HPLC method was validated for the determination of ASL in biological matrix. The limit of quantification (LOQ) (i.e., 0.1 μg/ml) was determined as the ASL peak was identifiable and reproducible with a precision of less than 20%. A calibration curve was prepared using six calibration standards (0.1–10 μg/ml, 5 μg/ml I.S.). Intraday and interday accuracy and precision were determined by analysis of the 0.1, 5 and 10 μg/ml concentrations. ASL relative recoveries from plasma and tissues were determined by comparing the concentration of extracted samples (0.1, 5 and 10 μg/ml) with the unextracted standards containing the same amount of the analyte. In all the cases five replicate samples were determined.

2.8. Pharmacokinetics and statistical analysis

Pharmacokinetic analysis was carried out using non-compartmental analysis with WinNonlin version 5.0. The area under the plasma concentration-time profiles (AUC), the distribution ($t_{1/2\alpha}$) and elimination half-life ($t_{1/2\beta}$), the mean residence time (MRT), the volume of distribution at steady state (V_{ss}), and total plasma clearance (CL) were calculated. The areas under the tissue distribution curves were calculated by the log-linear trapezoidal method. Statistical significance on pharmacokinetic parameter differences among the treatment groups were analyzed by Student's *t*-test using SigmaStat 3.5 and statistical significance was defined by $P < 0.05$.

3. Results

3.1. ASL nanosuspension

Particle size following different size-reduction steps and in lyophilized powder following water re-dispersion were determined by the DLS technique (Table 1). Un-milled ASL was

Table 1
Effect of milling operation on particle size of asulacrine.

Milling operation	d(0.5) μm	d(0.9) μm
Un-milled ASL	39.6 ± 1.2	55.3 ± 1.3
Ultra-turrax milling	0.379 ± 0.1	7.535 ± 0.02
Pre-milling	0.230 ± 0.02	2.324 ± 0.01
High pressure homogenization (20 cycles at 1500 bar)	0.133 ± 0.02	0.702 ± 0.02

The values are shown as mean particle size ± S.D., $n = 3$.

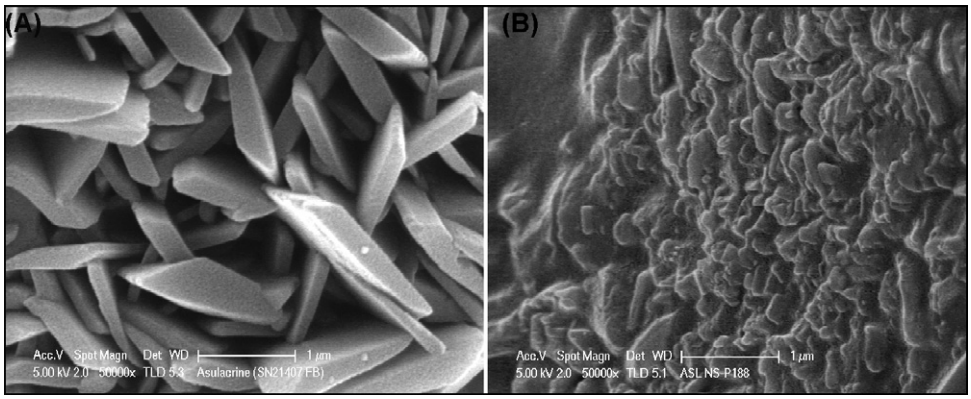

Fig. 1. Scanning electron micrographs of asulacrine: (A) Un-milled asulacrine and (B) nano-sized asulacrine. Magnification: 50,000× and scale bar 1 μm.

characterized by relatively large particles with a d(v; 0.5) about 39.6 μm (Table 1). Ultra-turrax and pre-milling operations were employed to obtain the relatively smaller size particles prior to high pressure homogenization (i.e., 25 μm at 22,000 psi) (Muller et al., 2001). These operations were only effective as preliminary size-reduction steps, and a high pressure homogenization with 20 cycles at 1500 bar pressure was necessary to obtain nanoparticles with a d(v; 0.5) of around 133 nm and d(v: 0.9) of around 702 nm, respectively (Table 1).

A surfactant or polymer was necessary for nanoparticles stabilization after the high pressure homogenization, and poloxamer 188 at 1% (w/v) was found to be suitable for this purpose. After the homogenization step, the nanosuspension was immediately lyophilized to obtain the dried ASL nanoparticles as this maintained both the physical and chemical stability of the drug. There was no significant change in the ASL nanoparticle size after re-dispersion of the lyophilized particles in glycerin–water. The particle morphology assessment by SEM helped in understanding the morphological changes that a drug might undergo when subjected to size-reduction process (Patravale et al., 2004). As seen from Fig. 1, the high pressure homogenization resulted in the formation of smaller ASL particles.

3.2. Crystalline state evaluation

Crystalline state evaluation was carried out after high pressure homogenization process. As can be seen from the DSC thermograms (Fig. 2), the peaks for un-milled ASL and ASL nanoparticles were nearly identical, with a sharp melting point of 281 °C. In addition, the PXRD analysis (Fig. 3) showed that the diffraction pattern was preserved for the ASL nanoparticles, and indicated that the crystalline state was apparently unaltered following the homogenization operation.

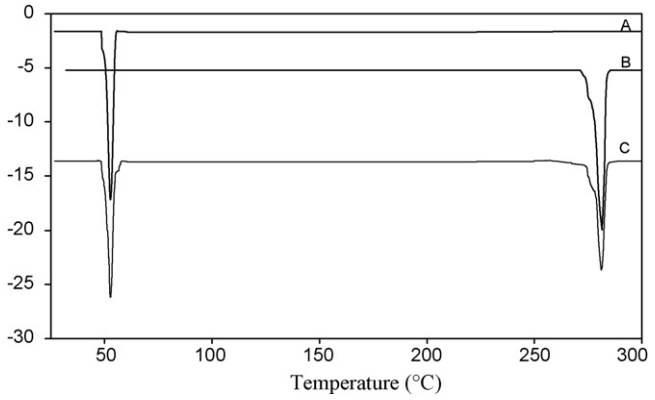

Fig. 2. Overlaid DSC thermograms: (A) poloxamer 188; (B) un-milled asulacrine; and (C) asulacrine nanosuspension.

3.3. Solubility and dissolution

Un-milled ASL showed negligible solubility in PBS pH 7.4. In contrast, ASL nanoparticles showed enhanced solubility (42 ± 3 μg/ml), attributed to the nano-sized ASL. As can be seen in Fig. 4, the solubility of ASL was a function of particle size. When the particle size was decreased following successive size-reduction steps, the solubility increased, with the highest solubility achieved with a particle size of d(v; 0.5) 133 nm.

The dissolution profiles for ASL in PBS pH 7.4 after turrax milling and high pressure homogenization were compared (Fig. 5). A 42% drug dissolution was achieved after the high pressure homogenization compared to 6% after turrax milling.

3.4. Stability of nanosuspension

The physical stability of the lyophilized ASL nanosuspension was evaluated over 3 months at 4 and 25 °C. During this storage period, the particle size did not change, and ASL stability was maintained, with more than 99% of ASL remaining in the nanosuspension, indicating that the lyophilized product has a shelf-life of at least 3 months.

3.5. Pharmacokinetics and tissue distribution

The performance of the analytical method for ASL determination in biological matrix was established (Ganta et al., 2008). The LOQ for the quantification of ASL in plasma was 0.1 μg/ml with a precision of 10.2%, and the linear range was 0.1–10 μg/ml (r^2 – 0.999). Intraday and interday precision was 7.8% and 6.9%, respectively, and intraday and interday accuracy was ±4.7% and ±8.3%, respectively. These values were within the limits (<15%) specified for interday and intraday precision and accuracy. ASL relative recoveries from the plasma and tissue (liver, kidney, lungs and heart) were 102.8% and 95.1% to 101.2%, respectively.

I.v. administration of both ASL solution and ASL nanosuspension (ASL-NS) was well tolerated by all mice. The plasma concentration–time profiles of ASL obtained are shown in Fig. 6 and the corresponding pharmacokinetic parameters in Table 2. Although both plasma profiles declined in a bi-exponential fashion, their profiles were markedly different with ASL-NS exhibiting a very rapid distribution phase ($t_{1/2\alpha}$ = 0.1 ± 0.01 h compared

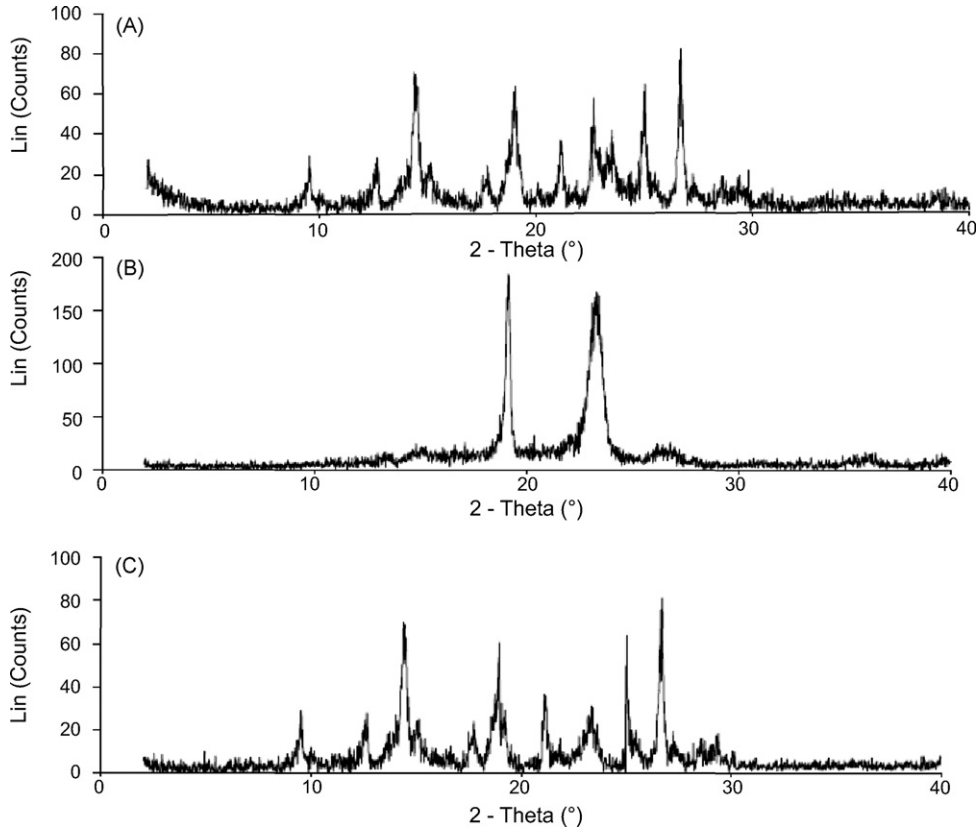

Fig. 3. PXRD diffractograms: (A) un-milled asulacrine; (B) Poloxamer 188; and (C) asulacrine nanosuspension.

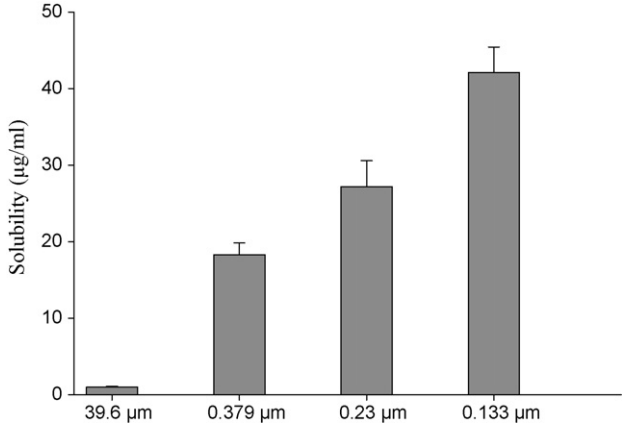

Fig. 4. Solubility as a function of particle size following successive size-reduction steps for asulacrine. Data are mean ± S.D., $n = 3$.

Table 2
Plasma pharmacokinetic parameters after i.v. administration of ASL solution and ASL-NS at a dose of 30 mg/kg of asulacrine.

Pharmacokinetic parameters	ASL	ASL-NS
C_{max} ($\mu g\,ml^{-1}$)	18.3 ± 1.0	12.2 ± 1.3
$AUC_{0-\infty}$ ($\mu g\,ml^{-1}\,h$)	46.4 ± 2.6	18.7 ± 0.5
MRT (h)	3.5 ± 0.2	9.6 ± 0.3
$t_{1/2\alpha}$ (h)	0.9 ± 0.16	0.1 ± 0.01
$t_{1/2\beta}$ (h)	2.7 ± 0.2	6.1 ± 0.1
CL ($l\,h^{-}\,kg^{-1}$)	0.6 ± 0.04	1.6 ± 0.04
V_{ss} ($l\,kg^{-1}$)	2.5 ± 0.1	15.5 ± 0.6

Data are shown as mean ± S.D., $n = 3$. Statistically significant when the pharmacokinetics parameters of ASL-NS compared with ASL at $P < 0.01$.

to ASL solution ($t_{1/2\alpha} = 0.9 \pm 0.16$ h). In contrast the elimination phase ($t_{1/2\beta}$) for the ASL-NS formulation was significantly ($P < 0.01$) longer ($t_{1/2\beta} = 6.1 \pm 0.1$ h) compared to that for ASL ($t_{1/2\beta} = 2.7 \pm 0.2$ h). The peak plasma concentration (C_{max}) achieved after ASL (18.3 ± 1.0 μg/ml) was significantly greater ($P < 0.01$) than that observed after ASL-NS (12.2 ± 1.3 μg/ml). Similarly the plasma $AUC_{0-\infty}$ for ASL solution (46.4 ± 2.6 $\mu g\,ml^{-1}\,h$) was approximately 2.5-fold greater than that for ASL-NS (18.7 ± 0.5 $\mu g\,ml^{-1}\,h$), but overall the mean residence time (MRT, 9.6 ± 0.3 h) for the ASL-NS formulation was considerably longer (2.7-fold) than that observed for the ASL solution. In mouse plasma, ASL was measurable at 13 h post injection of ASL-NS, but only up to 8 h after i.v. ASL solution.

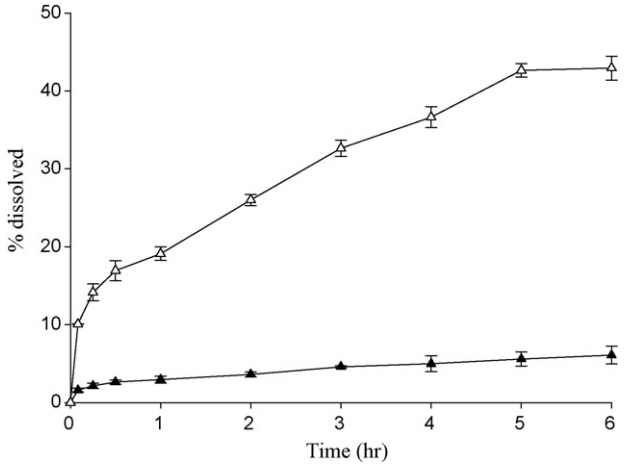

Fig. 5. Dissolution profiles for asulacrine following ultra-turrax (▲) and high pressure homogenization (△) milling. Data are mean ± S.D., $n = 3$.

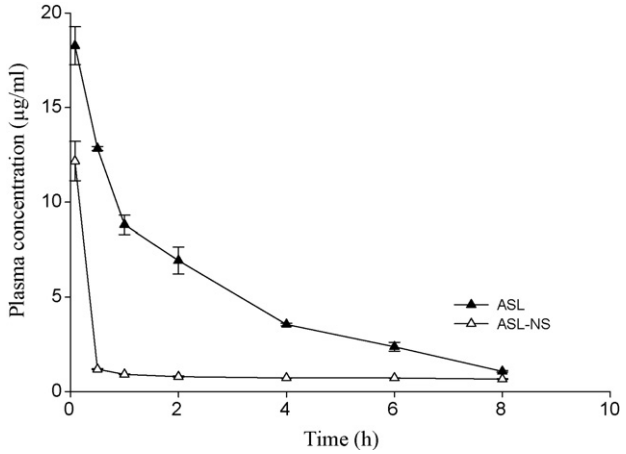

Fig. 6. Plasma concentration–time curves for asulacrine solution (ASL) and asulacrine nanosuspension (ASL-NS) after 30 mg/kg asulacrine i.v. in mice. Data are mean ± S.D., $n = 3$ mice.

Thus it is apparent that the ASL-NS formulation maintained lower plasma ASL concentrations but for a longer duration compared to the ASL solution.

In contrast to the plasma profiles, in all tissues (except the heart), significantly higher ASL concentrations were observed in mice administered the ASL-NS compared to the ASL solution ($P < 0.001$) (Fig. 7). The increase in $AUC_{0-\infty}$ ranged from 1.5-fold in the kidney to 10.4-fold in the liver, whereas the heart experienced a 16% reduction in its exposure to ASL after the nanosuspension formulation.

4. Discussion

Nanosuspensions are useful injectable dosage forms for poorly soluble drugs (Muller and Peters, 1998; Peters et al., 2000; Rabinow, 2004). High pressure homogenization is often used in the production of such nanosuspensions (Muller and Peters, 1998; Patravale et al., 2004; Rabinow, 2004). Stabilization of the nanoparticles in a nanosuspension form requires a stabilizer that binds onto the particle surface (Muller and Peters, 1998; Patravale et al., 2004; Rabinow, 2004). Poloxamers adsorb strongly onto the surface of hydrophobic nanoparticles via their hydrophobic polyoxypropylene centre block and have been shown to be quite successful in regard to nanoparticles stabilization (Storm et al., 1995). The particle size decreased in successive milling operations and the final nano-ranged particles were reached at high homogenization of 20 cycles and pressure at 1500 bar. In addition to particle size reduction, high pressure homogenization also permit rapid stabilization of the particles by allowing contact and binding of the stabilizers to the newly formed surfaces (Muller and Peters, 1998; Rabinow, 2004). Poloxamer 188, a non-ionic block polymer was used to stabilize the ASL nanoparticles.

Nanosuspension was lyophilized to obtain the dried ASL nanoparticles. Fig. 1B indicates that ASL nanoparticles were aggregated due to the water-removal (lyophilization). However, there

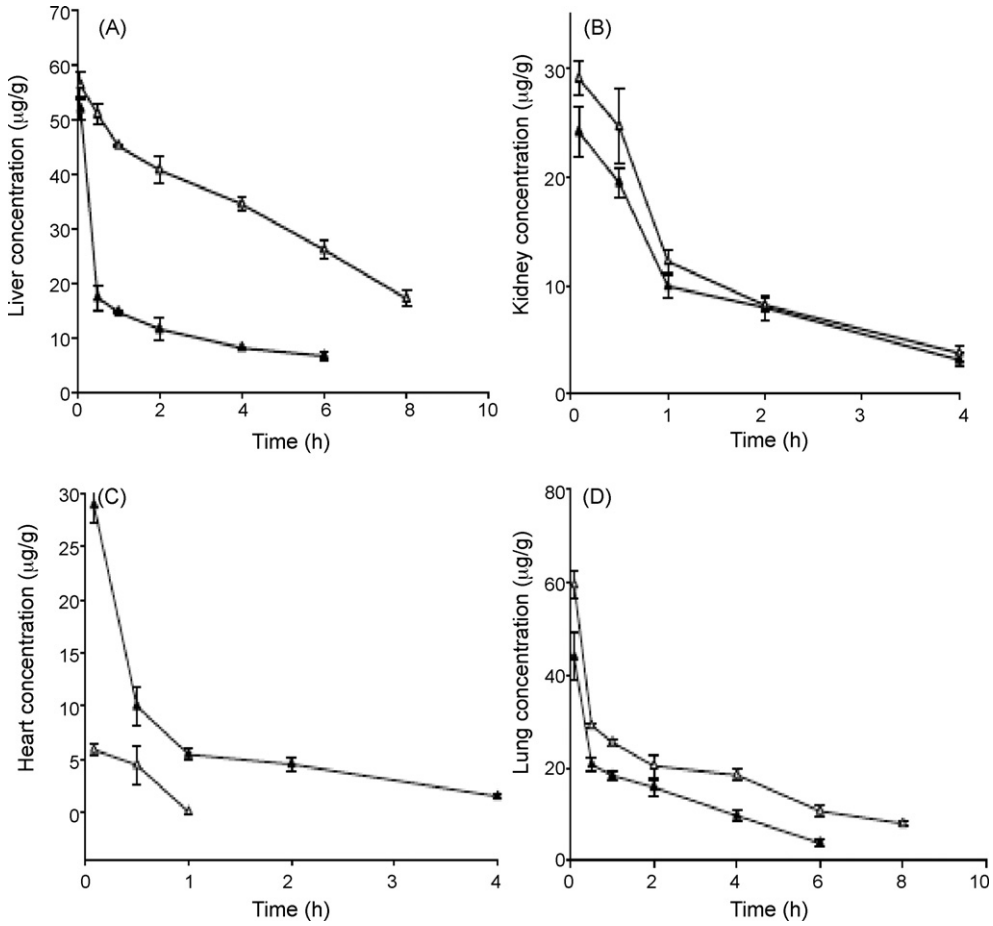

Fig. 7. Tissue distribution curves of asulacrine solution (▲) and asulacrine nanosuspension (△) after 30 mg/kg asulacrine i.v. in mice. (A) Liver, (B) Kidney, (C) Heart, and (D) Lungs. Data are mean ± S.D., $n = 3$ mice.

was no change in particle size measurements before and after lyophilization process.

DSC (Fig. 2) and PXRD (Fig. 3) profiles of ASL nanoparticles were not affected, indicating that the crystalline state of ASL appeared to be unaltered following the homogenization operation, which is important for long-term stability. Dissolution rate was increased with ASL nanoparticles, as 42% of the drug was dissolved in following 6 h from high pressure homogenized ASL compared to only 6% for ultra-turrax milled ASL. Although, the dissolution enhancement is clearly shown, it is still limited. Similarly, solubility enhancement also was observed with ASL nanoparticles.

The plasma pharmacokinetics of ASL when given in the nanosuspension formulation were markedly different compared to the ASL solution. The *in vivo* properties of a nanosuspension formulation strongly depend on the nanoparticle size, dissolution rate, and nature and density of the coating (Rabinow, 2004). Particles that dissolve rapidly in the blood would be expected to exhibit similar pharmacokinetic behavior to a drug in solution form. This was observed with flurbiprofen nanosuspension which had similar pharmacokinetics and tissue distribution as a flurbiprofen solution after i.v. administration in rats (Clement et al., 1992). This was thought to be due to the rapid dissolution of the flurbiprofen nanoparticles in the blood stream.

However the *in vitro* dissolution results (Fig. 5) indicated that the ASL nanoparticles may dissolve in the blood rather slowly, thus maintaining concentrations for a longer duration. There is evidence that when the dissolution of the nanosuspension is not instantaneous, there is less toxicity associated with it, thus enabling higher loading with safety (Boedeker et al., 1994). Although the plasma AUC of ASL nanosuspension was 40% of the AUC of the ASL solution, the plasma profiles indicated that the nanosuspension formulation maintained low plasma drug for a longer period of time. This effect might help to overcome the dose-limiting toxicity of ASL, which is associated with peak ASL concentrations (Hardy et al., 1988).

The pharmacokinetic profile in mice after i.v. administration of ASL nanosuspension resulted in a C_{max} which is 66% of that observed after ASL solution, and was followed by a rapid drop in plasma concentration to <1 μg/ml by 30 min. We suggest that this may be due to the rapid uptake of rather slowly dissolving ASL nanoparticles by the reticulate endothelial system (RES). Previous studies have shown that slow dissolving nanocrystals are taken up by the phagocytic cells of the mononuclear phagocyte system (MPS) (Gao et al., 2008; Moghimi et al., 2001), primarily the Kupper cells in the liver, spleen and lungs. As the phagocytoized drug particles are subjected to the reduced pH of phagolysosomes (Mukherjee et al., 1997), their pH-dependent solubility profile might permit dissolution of the compound. Their lipophilic character might permit passage through the phagolysosomal membrane, and as a result they could leave the cellular vesicle, enter the cytoplasm, and then exit the cell by diffusing down the drug concentration gradient (Rabinow, 2004). This effect will result in a pharmacokinetic profile with significantly reduced C_{max}, but quite prolonged $t_{1/2}$. This can be very advantageous for certain drug classes, for which toxicity is mediated by peak plasma values, but for which efficacy is driven by AUC, as in the case of triazole antifungals (Andes, 2003).

The ASL nanocrystals in the phagocytic cells might slowly dissolve and diffuse into the blood circulation to maintain blood concentrations for a longer duration. This could be the reason that after ASL nanosuspension is given to the mice, a low ASL concentration was observed for prolonged time. Higher plasma clearance and remarkably increased tissue concentrations could also support rapid clearance of ASL nanosuspension from the blood circulation by the RES. Despite the enhanced plasma clearance, a longer elimination half-life for ASL nanosuspension was observed, likely due to the enhanced distribution (6-fold) of the ASL-NS out of the bloodstream and uptake into the tissues such as the liver, kidney and lungs. PEG-modification of the surface of slowly dissolving drug crystals could reduce the macrophage uptake as observed with nanoparticles (Shenoy et al., 2005). This would increase circulation time, and allow the particles to leak out of discontinuities in tumour vasculature. This enhanced accumulation via the EPR effect results in passive targeting (Maeda and Matsumura, 1989). Therefore, the PEG-modification of ASL nanocrystals would avoid macrophage uptake and allow for longer duration in the blood circulation. As a consequence enhanced tumour accumulation of the nanocrystals may occur.

For ASL-NS, the drug nanocrystals could circulate in the blood as submicron particles for a certain time period. Then the nanocrystals might be recognized as foreign matter and rapidly cleared by phagocytic cells of MPS which are abundant in special tissues and organs, such as liver and lung (Gao et al., 2008; Moghimi et al., 2001). It was shown that the uptake of nanoparticles by RES organs following i.v. administration might take anywhere from a few minutes to hours, depending on particle size and composition (Manjunath and Venkateswarlu, 2005). Therefore the ASL nanocrystals in ASL nanosuspension had a markedly higher concentration compared with ASL solution in these organs. Meanwhile the drug concentration in kidney and heart decreased. Similar results were reported in literature (Peters et al., 2000).

In conclusion, the NS formulations of ASL, with the smaller particle size, can be effectively produced with the high pressure homogenization method. The particle size obtained was suitable for i.v. administration. To overcome the particle growth during long-term storage of NS formulations, lyophilization was carried out in order to assess the feasibility of transferring NS in a dry product. High pressure homogenization was shown to be a simple and adequate technique for drug particle size reduction and did not seem to alter the crystalline state of the drug, which should be highly relevant when considering drug stability during the storage. NS may give added value by allowing a reduction in either the dose or its frequency of administration. Moreover, a NS formulation may also reduce the risk of undesired adverse effects related to the initial plasma peak, without losing the high overall exposure. The pharmacokinetic profiles of ASL when given in the nanosuspension formulation were different compared to the ASL solution. In our future work, we will evaluate whether this change in ASL pharmacokinetics and tissue distribution will result in an increase in its anti-tumour activity.

Acknowledgements

The authors gratefully acknowledge the financial support provided by the UniServices, the University of Auckland, New Zealand. We would like to thank Elaine Marshall and Angela Ding, Auckland Cancer Society Research Centre, The University of Auckland, New Zealand for their support in animal experiments.

References

Andes, D., 2003. In vivo pharmacodynamics of antifungal drugs in treatment of candidiasis. Antimicrob. Agents Chemother. 47, 1179–1186.

Baguley, B.C., 1990. The possible role of electron-transfer complexes in the antitumour action of amsacrine analogues. Biophys. Chem. 35, 203–212.

Baguley, B.C., Denny, W.A., Atwell, G.J., Finlay, G.J., Rewcastle, G.W., Twigden, S.J., Wilson, W.R., 1984. Synthesis, antitumor activity, and DNA binding properties of a new derivative of amsacrine, N-5-dimethyl-9-[(2-methoxy-4-methylsulfonylamino)phenylamino]-4-acridinecarboxamide. Cancer Res. 44, 3245–3251.

Boedeker, B.H., Logeski, E., Kline, M., Haynes, D., 1994. Ultra-long duration local anesthesia produced by injection of lecithin-coated tetracaine microcrystals. J. Clin. Pharmacol. 34, 699–702.

Böhm, B.H., Muller, R.H., 1999. Lab-scale production unit design for nanosuspensions of sparingly soluble cytotoxic drugs. Pharm. Sci. Tech. Today 2, 336–339.

Buchmann, S., Fischli, W., Thiel, F.P., Alex, R., 1996. Aqueous suspension, an alternative intravenous formulation for animal studies. Eur. J. Pharm. Biopharm. 42, S10.
Cain, B.F., Atwell, G.J., Denny, W.A., 1975. Potential antitumor agents. 16. 4′-(Acridin-9-ylamino)methanesulfonanilides. J. Med. Chem. 18, 1110–1117.
Clement, M., Pugh, W., Parikh, I., 1992. Tissue distribution and plasma clearance of a novel microcrystalline-coated flurbiprofen formulation. Pharmacologist 34, 204.
Covey, J.M., Kohn, K.W., Kerrigan, D., Tilchen, E.J., Pommier, Y., 1988. Topoisomerase II-mediated DNA damage produced by 4′-(9-acridinylamino)-methanesulfon-m-anisidide and related acridines in L1210 cells and isolated nuclei: relation to cytotoxicity. Cancer Res. 48, 860–865.
Ganta, S., Paxton, J.W., Baguley, B.C., Garg, S., 2008. Development and validation of bioanalytical method for the determination of asulacrine in plasma by liquid chromatography. J. Pharm. Biomed. Anal. 46, 386–390.
Gao, L., Zhang, D., Chen, M., Duan, C., Dai, W., Jia, L., Zhao, W., 2008. Studies on pharmacokinetics and tissue distribution of oridonin nanosuspensions. Int. J. Pharm. 355, 321–327.
Hardy, J.R., Harvey, V.J., Paxton, J.W., Evans, P., Smith, S., Grove, W., Grillo-Lopez, A.J., Baguley, B.C., 1988. Phase I trial of the amsacrine analogue 9-({2-methoxy-4-[(methylsulfonyl)amino]-phenyl}]amino)-N,5-dimethyl-4-acridinecarboxamide (CI-921). Cancer Res. 48, 6593–6596.
Hintz, R.J., Johnson, K.C., 1989. The effect of particle size distribution on dissolution rate and oral absorption. Int. J. Pharm. 51, 9–17.
Jacobs, C., Muller, R.H., 2002. Production and characterization of a budesonide nanosuspension for pulmonary administration. Pharm. Res. 19, 189–194.
Lipinski, C., 2002. Poor aqueous solubility—an industry wide problem in drug discovery. Am. Pharm. 5, 82–85.
Lipinski, C.A., Lombardo, F., Dominy, B., Feeney, P., 1997. Experimental and computational approaches to estimate solubility and permeability in drug discovery and development settings. Adv. Drug Deliv. Rev. 23, 3–25.
Liversidge, G.G., Cundy, K.C., 1995. Particle size reduction for improvement of oral bioavailability of hydrophobic drugs: I. Absolute oral bioavailability of nanocrystalline danazol in beagle dogs. Int. J. Pharm. 125, 91–97.
Maeda, H., Matsumura, Y., 1989. Tumoritropic and lymphotropic principles of macromolecular drugs. Crit. Rev. Ther. Drug Carrier Syst. 6, 193–210.
Manjunath, K., Venkateswarlu, V., 2005. Pharmacokinetics, tissue distribution and bioavailability of clozapine solid lipid nanoparticles after intravenous and intraduodenal administration. J. Control. Release 107, 215–228.
Merisko-Liversidge, E., Sarpotdar, P., Bruno, J., Hajj, S., Wei, L., Peltier, N., Rake, J., Shaw, J., Pugh, S., Polin, L., Jones, J., Corbett, T., Cooper, E., Liversidge, G., 1996. Formulation and antitumor activity evaluation of nanocrystalline suspensions of poorly soluble anticancer drugs. Pharm. Res. 13, 272–278.
Moghimi, S.M., Hunter, A.C., Murray, J.C., 2001. Longcirculating and target-specific nanoparticles: theory to practice. Pharmacol. Rev. 53, 283–381.
Mukherjee, S., Ghosh, R.N., Maxfield, F.R., 1997. Endocytosis Physiol. Rev. 77, 759–803.
Muller, R.H., Jacobs, C., Kayser, O., 2001. Nanosuspensions as particulate drug formulations in therapy 'rationale' for development and what we can expect for the future. Adv. Drug Deliv. Rev. 47, 3–19.
Muller, R.H., Keck, C.M., 2004. Challenges and solutions for the delivery of biotech drugs—a review of drug nanocrystal technology and lipid nanoparticles. J. Biotechnol. 113, 151–170.
Muller, R.H., Peters, K., 1998. Nanosuspensions for the formulation of poorly soluble drugs: I. Preparation by a size-reduction technique. Int. J. Pharm. 160, 229–237.
Patravale, V.B., Date, A.A., Kulkarni, R.M., 2004. Nanosuspensions: a promising drug delivery strategy. J. Pharm. Pharmacol. 56, 827–840.
Peters, K., Leitzke, S., Diederichs, J., Borner, K., Hahn, H., Muller, R., Ehlers, S., 2000. Preparation of a clofazimine nanosuspension for intravenous use and evaluation of its therapeutic efficacy in murine *Mycobacterium avium* infection. J. Antimicrob. Chemother. 45, 77–83.
Rabinow, B.E., 2004. Nanosuspensions in drug delivery. Nat. Rev. Drug Discov. 3, 785–796.
Rosario, P., Claudio, B., Piera, F., Adriana, M., Antonina, P., Giovanni, P., 2002. Eudragit RS100 nanosuspensions for the ophthalmic controlled delivery of ibuprofen. Eur. J. Pharm. Sci. 16, 53–61.
Schneider, E., Darkin, S.J., Lawson, P.A., Ching, L.-M., Ralph, R.K., Baguley, B.C., 1988. Cell line selectivity and DNA breakage properties of the antitumour agent N-[2-(Dimethylamino)ethyl]acridine-4-carboxamide: role of DNA topoisomerase II. Eur. J. Cancer Clin. Oncol. 24, 1783–1790.
Shenoy, D., Little, S., Langer, R., Amiji, M., 2005. Poly(ethylene oxide)-modified poly(beta-amino ester) nanoparticles as a pH-sensitive system for tumortargeted delivery of hydrophobic drugs: part 2. In vivo distribution and tumor localization studies. Pharm. Res. 22, 2107–2114.
Sklarin, N., Wiernik, P., Grove, W., Benson, L., Mittelman, A., Maroun, J., Stewart, J., Robert, F., Doroshow, J., Rosen, P., Jolivet, J., Ruckdeschel, J.C., Robert, N.J., Velez-Garcıa, E., Bergsagel, D.E., Panasci, L.C., Merwe, A.M., Longueville, J.J., Leiby, J., Kowal, C.D., 1992. A phase II trial of CI-921 in advanced malignancies. Invest. New Drugs 10, 309–312.
Storm, G., Belliot, S.O., Daemen, T., Lasic, D.D., 1995. Surface modification of nanoparticles to oppose uptake by the mononuclear phagocyte system. Adv. Drug Deliv. Rev. 17, 31–48.